*17th World Conference on Earthquake Engineering, 17WCEE*
*Sendai, Japan - September 13th to 18th 2020*

# FE MACRO MODELING FOR IN-PLANE RESPONSES OF MASONRY INFILLED RC FRAME AND COMPARISON WITH EXPERIMENT

A.R. Bhuiyan[1] Z. Alam [2], D. Sen[3], F. Zahura [4] and A. M. Sikder[5]

[1]*Senior Consultant, Housing and Building Research Institute, Darus-Salam, Mirpur, Dhaka-1216, Bangladesh, E-mail: arbhuiyace@gmail.com and Professor, Department of Civil Engineering, Chittagong University of Engineering and Technology, Chittagong-4349 Bangladesh*
[2] *Junior Research Consultant, Housing and Building Research Institute, Darus-Salam, Mirpur, Dhaka-1216, Bangladesh, E-mail: zannatulbuet@gmail.com*
[3] *PhD student, Department of Architecture & Building Science, Tohoku University, E-mail: dsendip@rcl.archi.tohoku.ac.jp*
[4] *Associate Professor, Ahsanullah University of Science and Engineering,Tejgaon, Dhaka-1208, E-mail: fatema1777@gmail.com*
[5]*Senior Consultant, Housing and Building Research Institute, Darus-Salam, Mirpur, Dhaka-1216, Bangladesh, E-mail: sikder55@yahoo.com*

## *Abstract*

Bangladesh has a potential risk of future earthquakes as it is located in a tectonically active region close to the plate boundaries of the north moving Indian plate and the Eurasian plate to its north and east. A recent survey revealed that more than fifty percent of old RC and masonry buildings in major important cities, such as Dhaka, Chattogram and Sylhet are seismically vulnerable, which would require to be strengthened for future use conforming to the current building code. In this regard, proper assessment of the responses of building frames with/ without masonry infilled panel is a prerequisite for design of effective strengthening scheme suitable for a building. Incorporation of masonry infilled panel as structural member in seismic assessment of the building frames is one of the major challenges. The present study carried out numerical analysis, using a finite element package capable of calculating the finite deformation behavior of space frames under static or dynamic loading, taking into account both geometric nonlinearities and material inelasticity, of a 1:2 scale single-span single-story masonry infilled RC frame with aspect ratio of 0.79 and compared with experiment. The masonry infilled frame, as prepared using low strength concrete and cement mortar practiced in most of the old buildings of Bangladesh, was subjected to static cyclic loading with storey drift ranging from 0.05 % to 3.0%. To the end, the RC frame was modeled using inelastic beam-column elements and the masonry panel was modeled using the macro model [1]. Each panel was characterized by six strut members; each diagonal direction attributes two parallel struts to transmit axial loads across two opposite diagonal corners and a third one to carry the shear from the top to the bottom of the panel. The axial load struts used the masonry strut hysteresis model, while the shear strut used a bilinear hysteresis model. The numerical responses as obtained from FE macro model were compared with the experiment illustrating a good conformity with experiments in terms of lateral load vs. storey displacement behavior and hysteresis energy for the given boundary conditions. In addition, a parametric study was carried out to evaluate the sensitivity of the numerical results to the model parameters, particularly the empirical parameters and it showed a visible effect on the global response of the study frame.

*Keywords: FE macro modeling; inelastic beam-column; strut hysteresis model; bilinear hysteresis model; geometric nonlinearity and material material inelasticity*



## 1. Introduction

Unreinforced masonry infilled RC frames are a widely used structural system. The damages observed during past earthquakes highlight the negative effects of masonry infill panel on the seismic performance of structures. The seismic performance evaluation of masonry infilled RC frames has been a prevalent challenge for the last few decades. It has been observed that masonry infills are mostly used as interior partition walls and external walls in building according to the requirement of the usage. But they are seldom used in numerical analysis. The main reason for not including is complexity of analytical models for infill panel and not adequate knowledge. As a result, infilled wall is often treated as nonstructural elements and is omitted in the analysis models. Recent studies [2-8] have shown that the use of masonry infill panel has significant effect not only on the strength and stiffness but also on the energy dissipation mechanism of the overall structure. Neglecting the effects of masonry infill can lead to inadequate assessment of structural damage of infilled frame structures subjected to intense ground motions.

In order to fully comprehend the behavior of infill panel and its modes of failure, several analytical models have been proposed by researchers around the world. These models can be classified into two main groups, namely micro-models (local) and macro-models (simplified). Micro-models are based on the nonlinear finite element method and strive to provide an accurate representation of the frame-infill interaction at the local level. Different elements were used to model this approach such as beam elements for surrounding frame, plane frame element for representing infill and interface element for frame and panel interaction. For further detail on micro-models based on finite element approach, readers can refer to the works of Mallick and Severn [2], Mehrabi and Shing [3], Lotfi [4], Khair [5], etc. On the other hand, macro-models utilize the "equivalent truss" idea to provide a simple tool, capable to describe the global response of the masonry infill panel and its interaction with the peripherally bounding RC frame. Several studies have been conducted in order to define the appropriate modeling configuration, the properties, and the constitutive law of the equivalent struts or by developing appropriate constitutive laws to describe the hysteretic behavior of the panel when subjected to cyclic loading. The works of Smith [6], Crisafulli [7], Skafida and Koutas [8] etc. can be referred to in this regard.

Summarizing the available solution mechanisms, it seems that even though the macro-modeling schemes are not capable of simulating in a detailed manner all the possible failure mechanisms encountered in infilled frame structures, the limited computational effort required for their implementation makes them the best alternative, especially when analyzing large structures. The aim of this paper is to employ the macro-based modeling approach for the infilled panel in assessing the in-plane behavior of masonry infilled RC frame. The modeling scheme for the masonry panel presented herein primarily constitutes the "equivalent-truss" approach, originally developed by Crisafulli and Carr [1] with modification of the connections between the frame and masonry panel. The rigid connection as considered in the original model [1] is modified by a flexible connection using a linear spring element. The modified modeling approach of the masonry panel has been validated with experimental results of the masonry infilled RC frame subjected to in-plane cyclic quasi-static loading histories. Additionally, a parametric study has been conducted to clarify the influence of the various parameters on the overall structural response.

## 2. Analytical Modeling

### 2.1 Modeling scheme

A Finite Element software, SeismoStruct [9], capable of predicting the large displacement behavior of space frames under static and dynamic loadings taking into account both geometric nonlinearity and material inelasticity has been used in the current study. Macro-based FE modeling approach has been used in modeling the study frame, i.e. the masonry infilled RC frame. A four-node masonry panel element, initially developed and programmed by Crisafulli [7] has been employed for the modelling of the nonlinear response of infill panels in framed structures with a modification of the connections between the frame and masonry panel. As shown in Fig. 1, four internal nodes are employed to account for the actual points of contact



 



between the frame and the infill panel whilst four dummy nodes are introduced with the objective of accounting for the contact length between the frame and the infill panel. All the internal forces are transformed to the exterior four nodes where the element is connected to the frame. The rigid connection as considered in the original model [1, 7] is modified by a flexible connection. Linear spring elements have been used between the frame and infill panel nodes in order to take into account the fact that the infills are commonly not rigidly connected to the surrounding frames. Inelastic beam-column elements have been used to model the adjacent RC frame. A "force based beam-column" element with several integration points along its height has been used to model each beam/column member of the adjacent RC frame. Geometric dimension and analytical model of the stud frame is shown in Fig. 2.

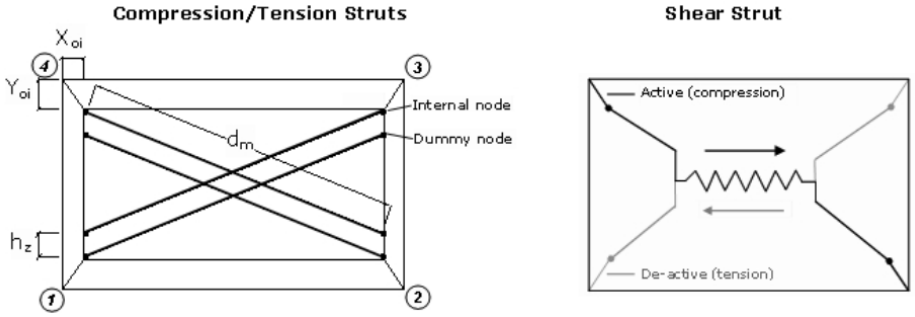


Fig.1- Schematic presentation of the masonry panel model [1]

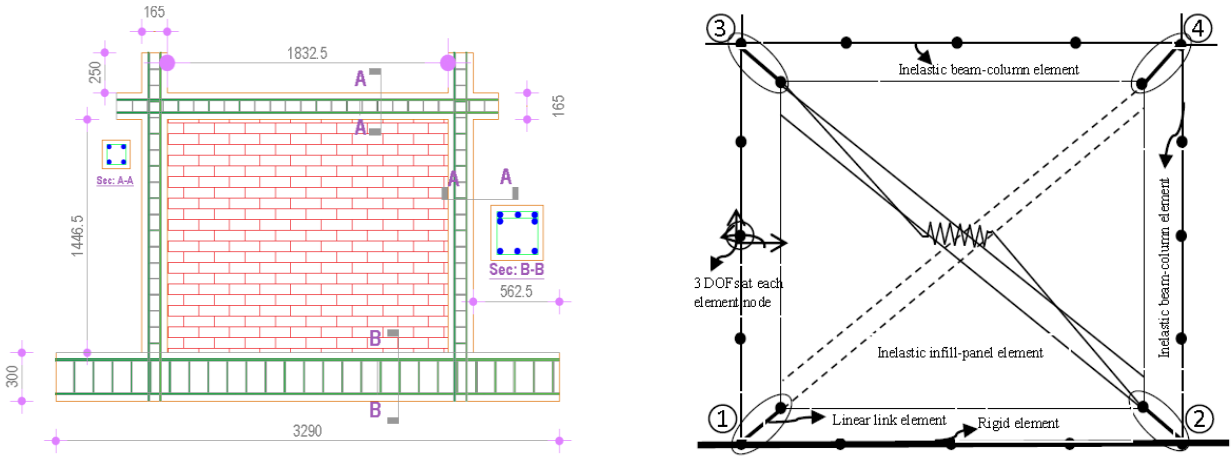


(a) (b)

Fig.2- (a) Physical model and (b) Analytical model of the study frame

## 2.2 **Constitutive material models**

### 2.2.1. *Concrete and reinforcing steel material models*

The inelastic fiber-based elements for concrete and reinforcing rebar have been employed for the numerical simulation of RC frame members. More specifically, "con-ma" and "stl-bl" as available in the software [9] were employed to model the concrete and the reinforcing rebar, respectively. The concrete model "con-ma" is a uniaxial nonlinear constant confinement model that follows the constitutive relationship proposed by Mander et al. [10]. The confinement effects provided by the lateral transverse reinforcement are incorporated through the rules proposed by Mander et al. [10], whereby constant confining pressure is assumed throughout the entire stress-strain range. The steel model "stl-bl" is a uniaxial bilinear stress-strain model with kinematic strain hardening, whereby the elastic range remains constant throughout the various loading



 



stages, and the kinematic hardening rule for the yield surface is assumed as a linear function of the increment of plastic strain.

### 2.2.2. *Cyclic compression/tension strut relation*

As shown in Fig. 1, each panel is represented by six strut members; each diagonal direction features two parallel struts to carry axial loads across two opposite diagonal corners and a third one to carry the shear from the top to the bottom of the panel. This latter strut only acts across the diagonal that is on compression. The axial load struts use the masonry strut hysteresis model, while the shear strut uses a dedicated bilinear hysteresis rule as described in Sub-Section 2.2.3.

Masonry infill strut model, developed and initially programmed by Crisafulli [7] has been used to describe the behavior of masonry under axial cyclic loading. The hysteresis rules describing the model can also be found in literature [1, 8]. The constitutive law for the axial cyclic behavior of the strut is expressed in terms of stress-strain relationships using six material parameters, namely,

(i) *initial modulus of elasticity*, $E_m$: The elastic modulus represents the initial slope of the stress-strain curve and its value exhibits a large variation since masonry is a composite material consisting of bricks and mortars, each of which features distinct properties.

(ii) *compressive strength*, $f'_m$: This compressive strength refers to the diagonal capacity of the infill panel not the standard compressive strength of the masonry. The widely accepted approach is to calculate a strength associated to each possible failure mechanism and assign the lowest obtained as the compressive strength. Four failure mechanisms, as discussed in different literatures, for example, Skafida and Koutas [8] and Bertoldi et al. [11] and the references cited therein, are stated in the following expressions:

Diagonal tension:

$$f'_m = \frac{0.6f_{ws} + 0.3\sigma_v}{\frac{w_{diag}}{D_p}}, \quad (1a)$$

Sliding shear:

$$f'_m = \frac{(1.2sin\theta + 0.45cos\theta)f_{wu} + 0.3\sigma_v}{\frac{w_{diag}}{D_p}}, \quad (1b)$$

Crushing in the corners:

$$f'_m = \frac{1.12f'_w sin\theta cos\theta}{K_1(\lambda_h)^{-0.12} + K_2(\lambda_h)^{-0.88}}, \quad (1c)$$

Diagonal compression :

$$f'_m = \frac{1.16f'_w tan\theta}{K_1 + K_2\lambda_h}, \quad (1d)$$

where $f_{ws}$ is the shear resistance under diagonal compression, $\sigma_v$ is the vertical compressive stress due to gravity loads, $f_{wu}$ is the sliding resistance of the mortar joints, $f'_w$ is the fundamental compression



 



resistance, $w_{diag}$ is the effective width of the diagonal strut and $D$p is the diagonal length of the panel. The parameters $K_1$and $K_2$ are expressed as a function of $\lambda_h$ as shown below:

Table 1-Parameters for the calculation of compressive strength of the strut [8]

| | $\lambda_h$ < **3.14** | **3.14** < $\lambda_h$ < **7.85** | $\lambda_h$ > **7.85** |
|---|---|---|---|
| $K_1$ | 1.3 | 0.707 | 0.47 |
| $K_2$ | -0.178 | 0.010 | 0.04 |

$\lambda_h$ is the relative panel-to-frame stiffness parameter, calculated as

$$\lambda_h = H \sqrt[4]{\frac{E_{m0}\, t_p \sin 2\theta}{4 E_c I_c H_p}}, \quad (2)$$

where $E_c$ and $I_c$ are the elastic modulus and the moment of inertia of the columns and $H_{panel}$ is the clear height of the panel.

(iii) *tensile strength*, $f_t^{'}$: The tensile strength represents the tensile strength of masonry or the bond strength of the interface between frame and infill panel.

(iv) *strain at maximum stress*, $\varepsilon_m^{'}$: This parameter represents the strain at maximum stress and affects the ascending branch of the stress-strain curve through modification of the secant stiffness.

(v) *ultimate strain*, $\varepsilon_{ult}$: This strain controls the descending branch of the stress-strain curve, modelled with a parabola so as to obtain better control of the strut's response.

(vi) *closing strain*, $\varepsilon_{cl}$: This parameter defines the strain at which the cracks partially close allowing compression stresses to develop.

In addition to these mechanical material parameters, a set of nine empirical factors associated exclusively with the hysteretic response need to be defined as proposed by Crisafulli [7] to fully characterize the hysteretic response of the panel as stated in Table 5. The feasible ranges of the empirical parameters can be found in literature, such as Crisafulli [7] and Skafida and Koutas [8].

### 2.2.3. *Cyclic shear spring relation*

The cyclic response of the shear spring is expressed in terms of a bilinear model as developed by Crisafuli [7]. The shear strength of a masonry panel results as the combination of two mechanisms, namely, bond strength and the friction resistance between the mortar joints and the bricks. In this case the shear behavior of masonry panel can be expressed by two hysteresis rules as proposed by Crisafuli [7].

### 2.2.4. *Cyclic linear spring relation*

From the construction practice of masonry infilled RC frames it is revealed that the RC frame and infill panel are not monolithically constructed. In order to take into account the fact that the infills are commonly not rigidly connected to the surrounding frame, linear link elements are used to model the connections between nosed of the RC frames and the infill panel. In this study the stiffness of the linear spring is considerad as 1 N/mm.

## 2.3 Geometric properties of the masonry panel

In addition to the above mentioned properties, a few geometric stiffness properties as stated below are needed to fully characterize the masonry panel model.



 



*i) Infill panel thickness:* it may be considered as equal to the width of the panel bricks alone or include also the contribution of the plaster

*ii) Out-of-plane failure drift:* it dictates the de-activation of the element, i.e. once the panel, not the frame, reaches a given out-of-plane drifts, the panel no longer contributes to the structure's resistance or stiffness.

*iii) Initial and reduced strut area:* the initial area of the panel is obtained as the product of the panel thickness and the equivalent width of the strut. The width of the strut varies between 10% and 40% of the diagonal of the infill panel [9]. The reduced strut area is taken, as percentage of the initial strut area, to take into account the fact that due to cracking of the infill panel, the contact length between the frame and the infill decreases as the lateral and consequently the axial displacement increases, affecting thus the area of equivalent strut.

*v) Equivalent contact length*: it is expressed as percentage of the vertical height of the panel, effectively yielding the distance between the internal and dummy nodes, and used so as to somehow take due account of the contact length between the frame and the infill panel.

### 2.4 Properties of the masonry panel

For the evaluation of the initial stiffness of the masonry panel, the following formula suggested by Bertoldi et al. [11] has been adopted

$$K_p = \frac{G_m A}{H_p} = \frac{G_m \left(L_p t_p\right)}{H_p} \quad , \tag{3}$$

where $L_p$ is the clear length of the panel; $H_p$ is the clear height of the panel; $t_p$ is the thickness of the panel and $G_m$ is the shear modulus of the masonry infill as determined using the masonry panel diagonal compression test [12].

The initial stiffness as expressed in the horizontal direction of the panel is shared between the diagonal strut and the shear spring according to the following expressions:

$$K_{spr,h} = \gamma_s K_p = \gamma_s \frac{G_m A}{H_p} \quad , \tag{4a}$$

$$K_{strut,h} = (1-\gamma_s) K_p = (1-\gamma_s) \frac{G_m A}{H_p} \quad , \tag{4b}$$

where $\gamma_S$ indicates the portion to the initial stiffness of the panel assigned to the shear spring.

## 3. Application of the Model

### 3.1 Experimental results

Experimental results of a 1:2 scale single-span single-story masonry infilled RC frame (study frame) with aspect ratio of 0.79, as carried out by Zahura et al. [13], were used for the purpose of comparison with the macro-based FE analysis results of the masonry infilled panel. The geometric and material of the frame specimen are given in Tables 2 and 3.

### 3.2 Numerical results

The results as obtained from the macro-based FE analysis of the study specimen are compared with experimental results in terms of base shear and inter-story displacement. The masonry infilled frame was subjected to static cyclic loading with storey drift ranging from 0.05 % to 3.0% as shown in Fig.3. The parameters assigned to the hysteresis models for the diagonal strut and shear spring of the masonry panel are given in Tables 4 and 5. The comparison of the model prediction and the experimental results is quantified



 



in terms of cumulative dissipated energy and the force based dimensionless index as described in the following sub-sections.

*i) Cumulative dissipated energy*: the prediction efficiency of an analytical model is checked by comparing the cumulative strain energy dissipated during each test with the dissipated energy obtained from the analytical model. The cumulative dissipated strain energy, *S,* at each loading step of the test is computed according to the following expression:

$$S_i = S_{i-1} + \frac{1}{2}(F_i + F_{i-1})(D_i - D_{i-1}), \tag{5}$$

where $S_{i-1}$ is the strain energy dissipated in the previous loading step, $F_i$ and $F_{i-1}$ are the base shear at two adjacent steps, $D_i$ and $D_{i-1}$ are the corresponding story displacements. The average error between the cumulative strain energy dissipated in the analytical model and the actual strain energy dissipated during the experiment is calculated as

$$Error(S) = \frac{\sum_{i=1}^{n}\left(\left|S_i^{anal} - S_i^{exp}\right|\right)}{\sum_{i=1}^{n}\left(\left|S_i^{exp}\right|\right)}, \tag{6}$$

Table 2- Geometric properties and reinforcement details of the specimen [13]

| Parameters | Unit | Value |
|---|---|---|
| Panel thickness, $t_p$ | *mm* | 125 |
| Clear length of the panel, $L_p$ | *mm* | 1832 |
| Clear height of the panel, $H_p$ | *mm* | 1440 |
| Width of the column, $b_c$ | *mm* | 165 |
| Depth of the column, $h_c$ | *mm* | 165 |
| Width of the top beam, $b_b$ | *mm* | 165 |
| Depth of the top beam, $h_b$ | *mm* | 165 |
| Flexural reinforcement of column, $A_{s,c}$ | - | 4-φ12 |
| Flexural reinforcement of top beam, $A_{s,b}$ | - | 4-φ12 |
| Shear reinforcement of column, $A_{sw,c}$ | - | Φ8@100 *mm* |
| Shear reinforcement of beam, $A_{sw,b}$ | - | Φ10@125 *mm* |

Table 3- Primary material properties of the specimen [13]

| Parameters | Unit | Value |
|---|---|---|
| Compressive strength of concrete, $f_c'$ | MPa | 18.85 |
| Yield strength of reinforcement, $f_y$ | MPa | 415.0 |
| Shear strength of masonry panel | MPa | 0.48 |
| Compressive strength of masonry panel, $f_m$ using Prism Test | MPa | 5.50 |



 



Table 4- Simulated material properties of the strut/spring element of the specimen

| Parameters | Unit | Value |
|---|---|---|
| Initial modulus of elasticity, $E_m$ | GPa | 0.40 |
| Compressive strength of masonry panel, $f_m^{'}$ | MPa | 1.00 |
| Tensile strength of masonry panel, $f_t^{'}$ | MPa | 0.06 |
| Strain at máximum compressive stress, $\varepsilon_m^{'}$ | - | 0.0012 |
| Ultimate strain, $\varepsilon_{ult}$ | - | 0.018 |
| Closing strain, $\varepsilon_{cl}$ | - | 0.0025 |
| Shear bond strength of masonry panel, $\tau_0$ | MPa | 0.10 |
| Friction coefficient, $\mu$ | - | 0.70 |
| Maximum shear stress, $\tau_{max}$ | MPa | 0.30 |
| Shear reduction factor, $\alpha_s$ | - | 1.50 |

Table 5- Simulated empirical parameters of the strut/spring element of the specimen

| Parameters | Value |
|---|---|
| Starting unloading stiffness factor, $\gamma_{un}$ | 35 |
| Strain reloading factor, $\alpha_{re}$ | 0.20 |
| Strain inflection factor, $\alpha_{ch}$ | 0.10 |
| Complete unloading factor, $\beta_a$ | 1.50 |
| Stress inflection factor, $\beta_{ch}$ | 0.90 |
| Zero stress stiffness factor, $\gamma_{plu}$ | 1.00 |
| Reloading stiffness factor, $\gamma_{plr}$ | 1.50 |
| Plastic unloading stiffness factor, $e_{x1}$ | 2.50 |
| Repeated cylic strain factor, $e_{x2}$ | 1.40 |

The cumulative strain energy dissipated in the analytical model is compared to the cumulative strain energy during the experiment of the study specimen. Moreover, the error in the dissipated strain energy as determined by Eq. (7) is used as a global measure of the accuracy of every numerical simulation.

*ii) Force based non-dimensional index*: the comparison of the model predictions and experimental results is evaluated via a force- based dimensionless index, *f*, computed as the fraction of the aforementioned difference in the base shear values to the maximum experimentally obtained base shear as

$$Index, f = \frac{\left|F_i^{anal}\right| - \left|F_i^{exp}\right|}{\left|F_i^{exp}\right|_{max}}, \quad (7)$$



 



where the maximum value of the experimental base shear is computed as the mean of the positive and negative shear forces. Four additional parameters are calculated to provide a more insight of the adequacy of the numerical simulation, such as a) the median of the positive $f$ values, offering an insight into the level of overestimation of the base shear; b) the median of the negative $f$ values, indicating the level of underestimation of the base shear; c) the maximum and minimum $f$ values giving an indication of the maximum error.

The experimental and analytical results as obtained for the study frame subjected to quasi static displacement history shown in Fig. 3 are presented in Figs. 4 to 7. The comparison of the analytically obtained responses of the study frame with the corresponding experimentally obtained responses appear to be in good agreement illustrating capturing capacity in both the shape of the hysteretic loops and resistance of the frame in loading and unloading branches as shown in Figs. 4 and 6.

The cumulative strain energy dissipated by the study frame as obtained from the analysis and experiment is presented in Fig. 5. As shown in Fig. 5, the analytical model generally overestimates the cumulative strain energy of the frame and the maximum error as computed using Eq. 6 gives 10.9%, which can be regarded as the acceptable difference [8, 14]. The fluctuation of index $f$ throughout the displacement history as shown in Fig. 7 gives the level of overestimation of the base shear as 7.3% of the maximum experimental base shear, while the level of underestimation is approximated as 4.9%, both indicating a slight deviation from the experimental results. The range of $f$-values (0.34, -0.27) implies that the analytical results exhibit relatively large differences from the experiment at some points of the response as indicated by circles in Figs. 6 and 7. These points are usually related to the initial phase of an unloading/reloading cycle, and they tend to reduce after a few cycles as highlighted by circles in Figs. 6 and 7.

### 3.3 **Parametric study**

A parametric study has been carried out to look into the sensitivity of the model parameters on the responses of the study frame. The study considered four parameters, such as the starting unloading stiffness factor, $\gamma_{un}$, the proportion of the initial stiffness assigned to shear spring, $\gamma_s$, the width of the strut diagonal, $w_{\text{diag}}$ and the plastic unloading stiffness, $e_{x1}$ as the remaining parameters have negligible effects on frame responses [14]. The parameters are individually varied, keeping all the other quantities constant to the value used in the calibrated model presented in the previous section. In order to quantify the effect of the parameters mentioned above on the frame responses, the error in cumulative strain energy (Eq. 6) and the index, $f$ (Eq.7) are computed and compared for all variations of the considered parameters. The results of this comparison are presented in Figs. 8(a) to 8(d). The horizontal axis presents the variation of the parameter under investigation, the left vertical axis presents four index $f$ values and the right vertical axis indicates the error in cumulative strain energy (%). The selected parameter-value used in the model presented in Section 3.2 is presented by a red dashed line as shown in Figs. 8(a) to 8(d).

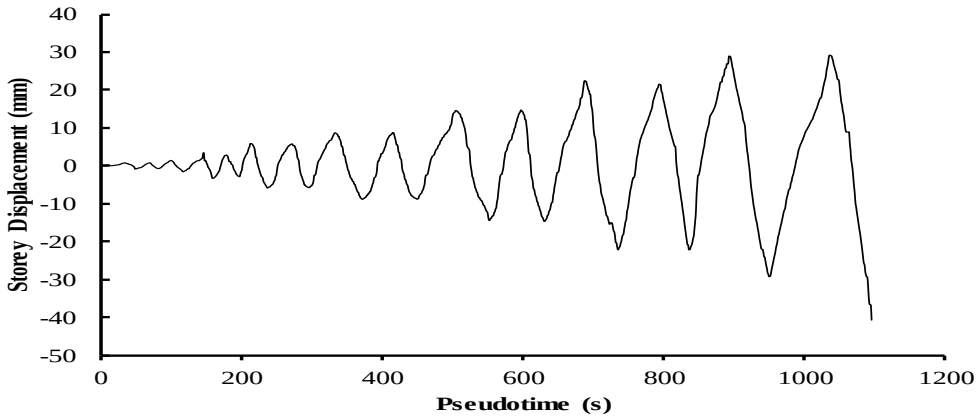


Fig.3- Time history of storey displacement applied to the study frame



 



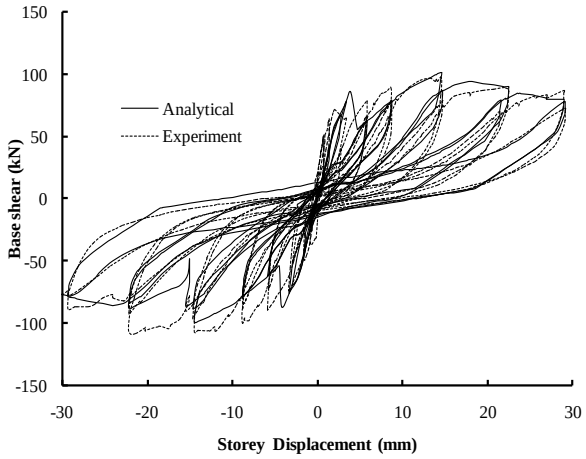


Fig. 4- Base shear vs. storey displacement of the study frame

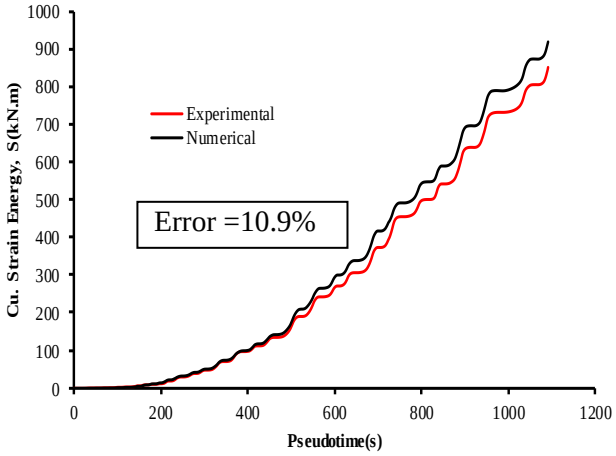


Fig.5- Cumulativa strain energy of the study frame

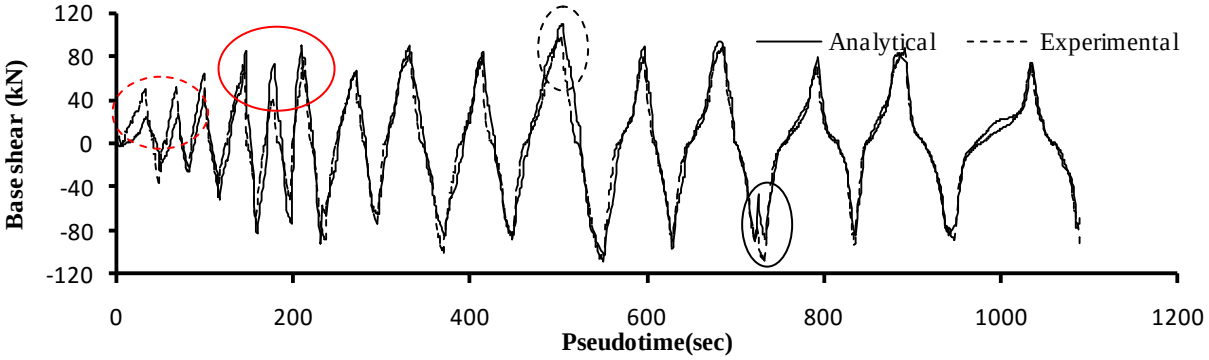


Fig.6- Time history of the base shear of the study frame

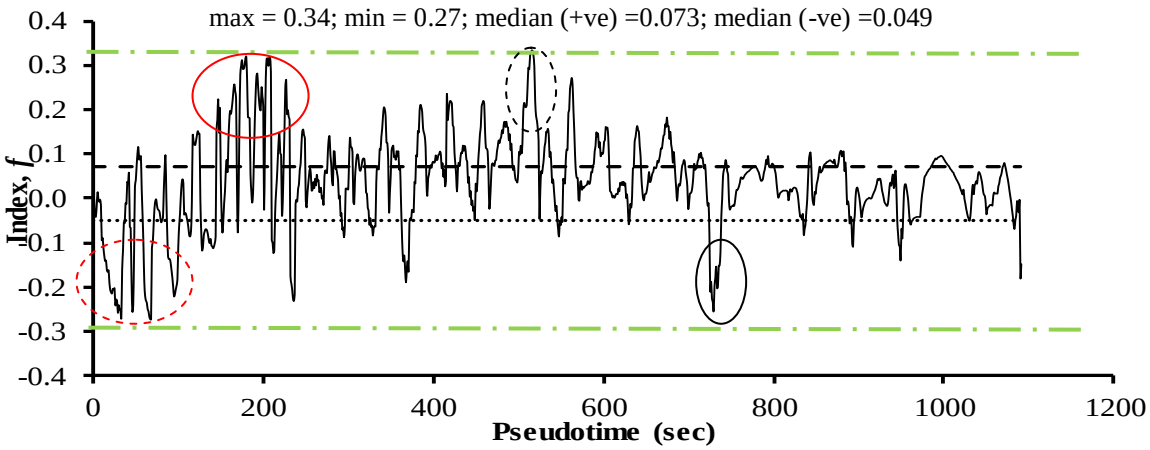


Fig.7-Variation of index *f* for the base shear of the study frame

Fig.8(a) presents the effect of the starting unloading stiffness factor $\gamma_{un}$ on the hysteretic response of the study frame illustrating a negligible influence on the global response of the frame in terms of index *f;* however, for the error in cumulative strain energy this parameter has notable effect on the response.



 



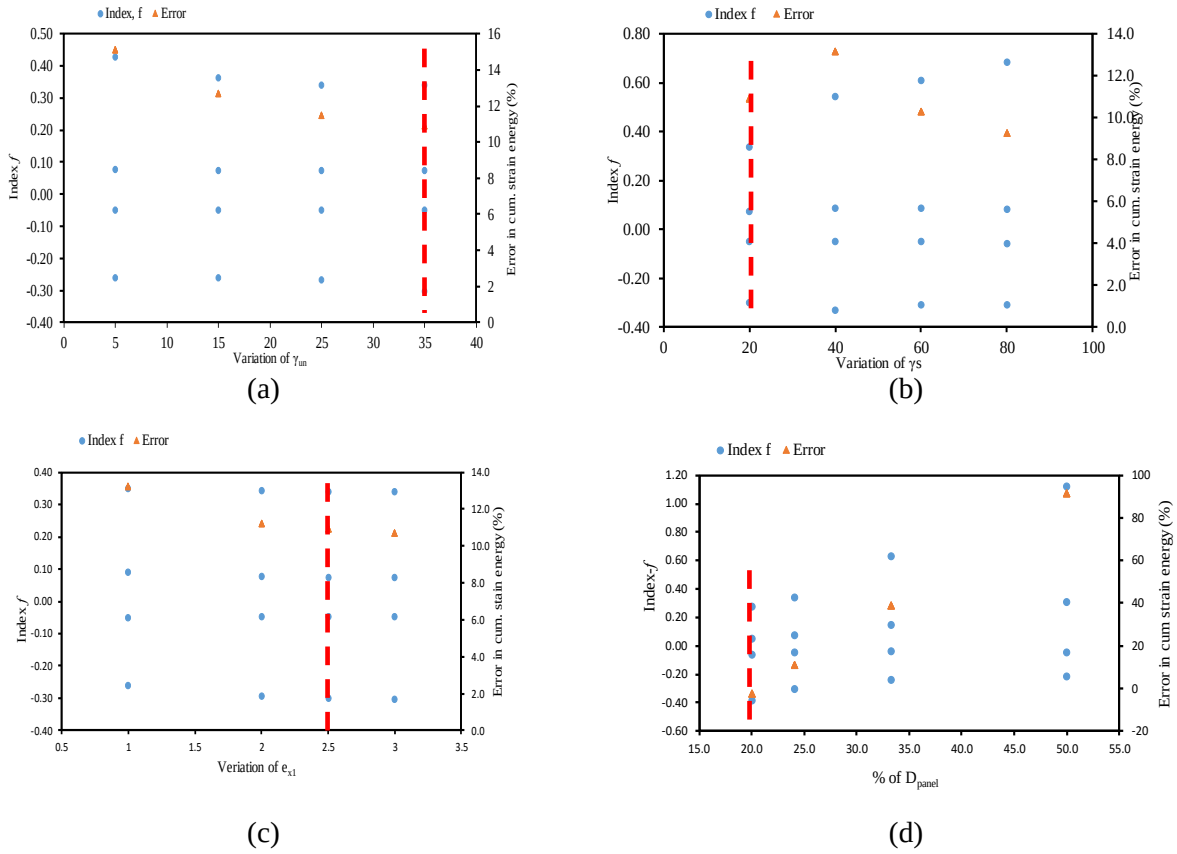


Fig.8-Parametric study of the study frame (a) starting unloading stiffness, (b) proportion of the initial stiffness assigned to shear spring, $\gamma_s$, (c) the plastic unloading stiffness, $e_{x1}$, (d) the effective width of the diagonal strut, $w_{diag}$ as % of $D_p$ (diagonal length of the panel). For clarity, the four values of index $f$ can be read from top to bottom as maximum, median (+ve), median (-ve) and minimum values as indicated by solid circle markers and the red triangular solid marker indicates the error in cumulative strain energy.

Parameter $\gamma_s$ seems to have a significant impact on the response of the frame as shown in Fig. 8(b). It can be observed that the level of underestimation varies from −30.0% for $\gamma_s$ = 0.2 to −33.0% for $\gamma_s$ = 0.8. The level of overestimation varies from 34% at $\gamma_s$ = 0.2 to 68% at $\gamma_s$ = 0.8. In case of the error in cumulative strain energy (%) it has been observed that for higher values of $\gamma_s$ the error in cumulative strain energy decreases. As shown in Fig. 8(c), the effect of plastic unloading stiffness, $e_{x1}$ on the frame response appears to be negligible in terms of index $f$; however, for the case of the error in cumulative strain energy this parameter has the significant effect. As expected, the reduction of the effective width of the diagonal strut seems to be one of the most influential parameters as revealed from Fig. 8(d) since it takes into account the relative panel-to-frame stiffness. The procedure has led to the use of $w_{diag}$ = 20 % $D_{panel}$ in the calibrated model that is verified by the parametric study.

## 4. Conclusions

This paper presents an approach for assessing the nonlinear response of a masonry infilled RC frame based on in-plane lateral loads. The macro model as proposed by Crisafulli and Carr [1] for the infill panel is modified for this purpose. The rigid connection, as considered by Crisafulli[7], between the frame and infill panel is replaced by a flexible connection using link element. The hysteretic models of the diagonal strut and shear spring comprise a number of mechanical and empirical parameters of the infill panel in addition to the link element properties used for the connection between the frame and the infill panel. Two quantities are



 



used to conduct the comparative assessment between the experimental and analytical results of the study frame: i) the average error in the cumulative dissipation energy obtained from experiment and analytical model and ii) the dimensionless index *f* which is computed from the difference of the base shear, at the same displacement level, divided by the experimentally obtained maximum base shear. From the comparison it has been seen that the analytical model can adequately predict the hysteretic response of the study frame as indicated by the values of the medians of positive *f* (7.3%) and negative *f* (4.9%) (Fig.7) and the average error in the cumulative strain energy (10.9%) (Fig. 8). In addition, a parametric study, carried out to evaluate the sensitivity of the numerical results to the model parameters, particularly the empirical parameters, shows noticeable effect on the global response of the study frame. In the current study, only single story - single bay masonry infilled RC frame without column's axial load due to gravity is considered; however, in the future work a multi-story-multi bay frame could be considered in the experimental plan for detail insight of the behavior of the frame subjected to lateral load coupled with axial load on the columns.

## 5. Acknowledgement

Authors sincerely express their whole-hearted gratitude to JICA/JST Science and Technology Research Partnership for Sustainable Development (SATREPS/TSUIB) project headed by Mohammad Shamim AKHTER (HBRI, Bangladesh) and Yoshiaki NAKANO (U. of Tokyo, Japan).

## 6. References

[1] Crisafulli FJ, Carr AJ (2007): Proposed macro-model for the analysis of inflled frame structures. *Bulletin of the New Zealand Society for Earthquake Engineering*, **40**(2), 69–77.

[2] Mallick DV, Severn RT (1969): Dynamic characteristics of infilled frames. *Proceedings of the Institution of Civil Engineers*, **39**, 261-287.

[3] Mehrabi AB, Shing PB (1997): Finite element modeling of masonry-infilled RC frames. *Journal of Structural Engineering*, **123**(5), 604-613.

[4] Lotfi HR, (1992): Finite element analysis of fracture of concrete and masonry structures. *PhD Dissertation*, University of Colorado, Boulder, Colorado.

[5] Khair MA (2005): Finite element analysis of unreinforced masonry walls subjected to inplane loads. *PhD Dissertation,* Bangladesh University of Engineering and Technology (BUET), Dhaka.

[6] Smith BS (1962): Lateral stiffness of infilled frames. *Journal of Structural Engineering*, **88**(6), 182-199.

[7] Crisafulli FJ (1997): Seismic behavior of reinforced concrete structures with masonry infills. . *PhD Dissertation,* University of Canterbury, Canterbury, New Zealand.

[8] Skafida SG, Koutas L (2014): Analytical modeling of masonry infilled RC frames and verification with experimental data. *Journal of Structures*, Hindawi Publishing Corporation, Article ID:216549, http://dx.doi.org/10.1155/2014/216549.

[9] SeismoStruct (2018): © 2002-2018 Seismosoft Ltd.

[10] Mander JB, Priestley MJN, Park R (1988): Theoretical stress-strain model for confined concrete, *Journal of Structural Engineering*, **114** (8), 1804-1826.

[11] Bertoldi SH, Decanini LD, Santini S, Via G (1994): Analytical models of infilled frames, *Proceedings of the 10th European Conference on Earthquake Engineering*, Vienna, Austria.

[12] ASTM E519/519M-10 (2010): Standard test method for diagonal tension (shear) in masonry assemblages.

[13] Zahura F, Sen D, Sabrin R, Das A, Uddin M, Tafheem Z, Khanam F, Alwashali H, Maeda M (2020): In-plane seismic performance of masonry infilled RC frame with and without ferro-cement overlay (Accepted), *Proceedings of the 17th World Conference on Earthquake Engineering*, Sendai, Japan.

[14] Smyrou E, Blandon CA, Antoniou S, Pinho R, Crisafulli F (2011): Implementation and verification of a masonry panel model for nonlinear dynamic analysis of infilled RC frames. *Bulletin of Earthquake Engineering*, DOI 10.1007/s10518-011-9262-6.



 